RSC Advances

ROYAL SOCIETY OF CHEMISTRY

www.rsc.org/advances

Journal Name

COMMUNICATION

A Simple Dimeric Model Accounts for the Vibronic ECD Spectra of Chiral Polythiophenes in their Aggregated States

Received 00th January 20xx,
Accepted 00th January 20xx

DOI: 10.1039/x0xx00000x

www.rsc.org/

Daniele Padula,[a] Fabrizio Santoro*[b] and Gennaro Pescitelli*[a]

Aggregates of chiral polythiophenes (PTs) show strong electronic circular dichroism (ECD) spectra with a unique vibronic structure. A computationally fast procedure, based on simple oligothiophene dimers as models of PT aggregates, is able to reproduce experimental vibronic ECD spectra of aggregated phases.

It is nowadays an established notion that the fundamental properties of materials based on π-conjugated polymers (CPs),[1] such as light absorption and emission, charge and exciton transport, and the performances of the devices constructed thereof, including light emitting diodes (LEDs), solar cells and field-effect transistors (FETs), depend not only on the molecular structure but also on the organization reached at various levels of hierarchy, up to the nano/mesoscale.[2,3] To design more efficient devices it is crucial to study and control the supramolecular structures at each level, and to understand the intermolecular interactions responsible for them.[4,5] Although chiral CPs represent a small fraction of all known systems,[6-8] chiroptical techniques, and especially electronic circular dichroism (ECD), have become a widespread tool for the investigation of CP aggregates. This is because, while isolated polymers and disordered supramolecular structures are often ECD-inactive, ECD is very sensitive to ordered (helical) assemblies,[9] particularly to the mutual orientation between conjugated polymeric chains, which is in turn strictly related to their transport properties.[5] It is noteworthy that in their recent review about pathway complexity and selection in the aggregation of π-conjugated materials,[10] Meijer and co-workers discuss ECD as the first and most used technique in the field. Despite these encouraging premises, the effective use of ECD in the study of chiral CPs is still restricted to detect and quantify aggregate formation, or to determine the handedness of helical aggregates – an application which is itself prone to error if based on merely qualitative assumptions.[9] The discovery of quantitative spectrum-to-structure relationships, which are the standard in many ECD applications,[11] is hampered in the field of CPs not only by the system complexity, but also by the complicated appearance of ECD spectra of CP aggregates. In fact, ECD signals allied with π-π* transitions of rigid or semi-rigid aggregates of π-conjugated polymers often manifest a distinct vibronic structure dominating their shape. This is especially true for chiral polythiophenes (PTs). Regioregular PTs represent perhaps the most successful family of CPs for optoelectronic applications.[12,13] Several chiral PTs have been synthesized and their ECD spectra reported.[14-37] In aggregated phases (solution aggregates promoted by low temperature or "poor" solvents, or thin films), ECD spectra of PTs are usually dominated by an exciton couplet feature[9] in the long-wavelength region corresponding to the first observed π-π* HOMO-LUMO transition of the PT core,[38] typically between 450-650 nm. Very interestingly, most of these ECD couplets (i.e. two bands close in energy with similar intensity and opposite sign) show a typical more or less pronounced vibronic structure,[14-29,39-41] although couplets with faint or missing vibronic structures are also encountered.[30-37,39,42-44]

Apart from the theoretical interest in vibronic excitonic ECD spectra,[45] it must be stressed that the coupling between delocalized electronic excitations (excitons) and intramolecular vibrations is a privileged mechanism for charge and energy transport in CPs. As such, the effects of electronic-vibronic coupling on absorption and emission spectra of CPs and particularly PTs have been studied extensively from both an experimental and theoretical viewpoint.[5,46-52] On the contrary, the vibronic features in ECD spectra of PTs have been considered only qualitatively.[16,20,25,28,29,53] Janssen and co-workers have studied the ECD spectra of chiral PTs in detail as a source of structural information,[17-19,23,26,54] however their quantitative treatment was focused on a small covalent bis(terthiophene) model and based on a semi-empirical calculation approach.[17,23] The most important conclusion from their series of papers is that, among the various possible

[a] Università di Pisa, Dipartimento di Chimica e Chimica Industriale Via G. Moruzzi 13, I-56124 Pisa, Italy. E-mail: gennaro.pescitelli@unipi.it
[b] Consiglio Nazionale delle Ricerche – CNR, Istituto di Chimica dei Composti Organo Metallici (ICCOM-CNR), UOS di Pisa, Via G. Moruzzi 1, I-56124 Pisa, Italy. E-mail: fabrizio.santoro@pi.iccom.cnr.it

Electronic Supplementary Information (ESI) available: Theoretical model; computational details; additional tables and figures. See DOI: 10.1039/x0xx00000x

sources of optical activity in aggregates of chiral PTs, a major role is played by the inter-chain exciton coupling established in helical packings of predominantly planar chains, rather than, for instance, from a helical conformation assumed in each chain (an intra-chain mechanism).[19]

Here, we demonstrate that the vibronic ECD spectra of chiral PTs may be properly taken into account – with the main aim to investigate the content of structural information they deliver – and satisfactorily reproduced by combining high level quantum mechanical calculations of vibronic ECD spectra[45] with simplified molecular models. The applicability and reliability of our method to conjugated polymers is verified here for the first time. We chose PTs as test case both for their importance and because oligothiophenes have been extensively studied with theoretical methods,[13] including time-dependent density functional theory (TDDFT) we also employed.[47,55]

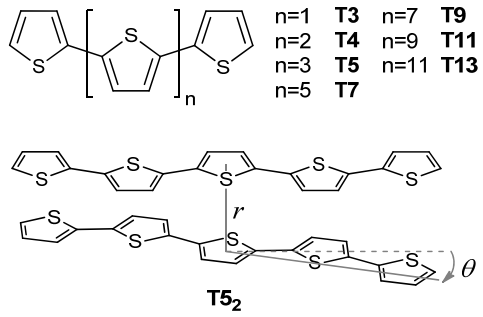

Scheme 1 Top: model oligothiophenes **Tn**. Bottom: dimer of **T5** showing definition of intermolecular plane-to-plane distance r and torsional angle θ.

The models for PT used here are oligothiophenes **Tn** composed of 3 to 13 thiophene units, and their dimers $\mathbf{Tn_2}$ (Scheme 1). The geometries of monomers **Tn** were optimized by DFT in C_{2h} symmetry (C_s for **T4**). The preferred supramolecular arrangement of PTs consists of all-trans conjugated chains placed anti-parallel to each other at distances starting from ≈4Å in the crystal state.[56] With the aim to mimic such arrangements and introduce chirality, we constructed the idealized geometries of the stacked dimers $\mathbf{Tn_2}$ by placing two monomers parallel to each other at variable distances r and twist angle θ (Scheme 1). Dimers were not re-optimized and distortions along the inter-ring torsions were not allowed.

As a first test of the consistency of our method, we considered the exciton coupling potential V_{12}. This was extracted from TDDFT calculations on the dimers at CAM-B3LYP/SVP level as half of the Davydov splitting between the first two excited states S1 and S2, which are essentially the linear combination of HOMO→LUMO excitations on the monomers (local excitations; the orbitals for $\mathbf{T7_2}$ are depicted in the Electronic Supplementary Information, ESI; Figure S1). This simple procedure takes into account also short-range interactions for symmetric dimers as those considered here.[57] Further details are given in the ESI, where (Tables S2) it is also shown that, at least for r =5 Å, the exciton couplings calculated by TDDFT are equivalent to those obtained assuming a Coulomb interaction between the transition densities and performing the related integral with the transition density cube method.[58] The dependence of V_{12} on the geometrical parameters and on the number of thiophene units is shown in Figure 1. As expected, V_{12} decreases with both r and θ (in the dipolar approximation $V_{12} \propto r^{-3}\cdot\cos\theta$). More interesting is the fact that, at fixed r, the $V_{12}(\theta)$ curves have a similar trend for all dimers but the coupling potential decreases upon increasing the chain length **n** (for **n**≥ 5). This is at odds with a simple dipolar model which predicts V_{12} to vary linearly with the dipolar (or oscillator) strength and then with **n** (see ESI, Figure S2). However, the dipolar approximation breaks down quickly as the chain length increases,[59] and for longer chains one should think at interchain interactions in terms of multiple interactions between different fragments on each chain, which eventually lead to an inverse coupling/length relationship, as observed experimentally and confirmed by theory.[5,46,59-63] Thus, the present TDDFT calculations on $\mathbf{Tn_2}$ dimers reproduce the expected trends.

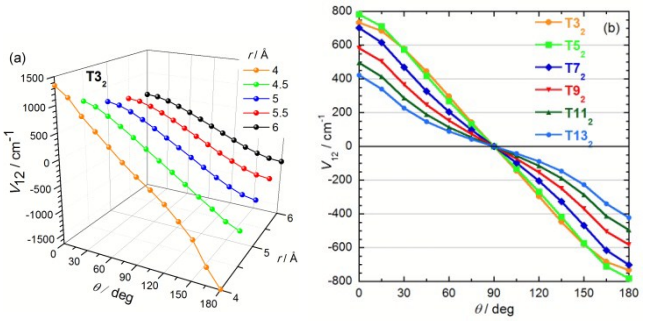

Fig. 1 (a) Coupling potential V_{12} calculated for dimer $\mathbf{T3_2}$ as a function of r and θ. (b) V_{12} calculated for dimers $\mathbf{Tn_2}$ as a function of θ at r= 5 Å. Calculations at TDDFT/CAM-B3LYP/SVP level.

Our method[45] for vibronic calculations in dimers is fully detailed in the ESI. Briefly, the ECD signal is obtained in a time-dependent formalism from the quantum dynamics on the coupled potential energy surfaces (PESs), corresponding to the local excitations on the two monomers. Such PESs are taken as harmonic and built from the ground-state equilibrium geometry and normal modes of the monomer **Tn** and from its equilibrium geometry in the excited state, obtained at CAM-B3LYP/SVP level of theory. In principle, the calculation of the dynamics on the coupled PESs is extremely challenging since it involves e.g. 126 nuclear coordinates for $\mathbf{T3_2}$, 294 for $\mathbf{T7_2}$, and 546 for $\mathbf{T13_2}$. The computation is performed by adopting a reduced number of effective vibrational modes, that is, linear combinations of the normal modes of the monomers rigorously defined to describe accurately the dynamics of the full-dimensionality system on a short timescale.[64,65] The approach also implies an accurate simulation of the ECD spectrum for a finite frequency resolution.[45] The number of necessary effective modes increases with the desired resolution of the converged spectrum. In this way, the traditional single-mode approximation is relieved[66] and the all-coordinates spectrum is obtained, but the procedure remains computationally feasible.

In Table 1 and Figure 2 we report the calculation results on dimers $\mathbf{Tn_2}$ at r= 5 Å and θ= 15°. A plane-to-plane distance of 5

Å is a reasonable compromise between the tight packing found in the solid state (r≈4Å)[56] and the larger spacing expected for "soft" solution aggregates and thin films, especially in the presence of branched pendants. Similarly, a small twist angle is a plausible choice because it allows the system to attain a well-defined chiral supramolecular assembly while preserving a sufficient amount of π-stacking between neighbouring chains.[67,68] The spectra and data for other dimers are given in the ESI, Figures S5-S12; dimer **T4$_2$** behaves as an intermediate between **T3$_2$** and **T5$_2$**, so no odd-even effect is detected. All convoluted spectra, obtained using a Gaussian bandshape with half width at half maximum HWHM= 450 cm^{-1}, were well converged with 6 effective modes, or even with 4 in most cases. On the contrary, the use of only 2 effective modes, namely one coordinate per monomer, afforded vibronic spectra far from convergence (ESI, Figures S5-S8). This is noteworthy because, as said above, most quantitative traditional treatments of vibronic excitonic ECD spectra are based on a single-coordinate approximation.[45,66,69]

Table 1 Main calculated data for **Tn** monomers and **Tn$_2$** dimers.

	T3	T5	T7	T9	T11	T13
E_v (cm^{-1}) [a]	29658	25118	23248	22278	21721	21361
V_{12} (cm^{-1}) [b]	660	700	610	505	415	340
ω_1 (cm^{-1}) [c]	1485	1489	1489	1487	1490	1490
λ_1 (cm^{-1}) [d]	2715	2558	2418	2352	2284	2221

[a] Vertical transition energy for the monomers, from TDDFT/CAM-B3LYP/SVP calculations on the monomers **Tn**. [b] Coupling potential, calculated from TDDFT/CAM-B3LYP/SVP calculations on the dimers **Tn$_2$**, at r= 5 Å and θ= 15 deg. [c] Frequency of the first effective mode on each monomer **Tn**, from our hierarchical description of the Hamiltonian. [d] Linear coupling of the first effective mode on each monomer **Tn**, from our hierarchical description of the Hamiltonian. This quantity is proportional to the displacement of the ground and excited equilibrium geometry of the monomer (see ESI).

The most striking observation from the calculated vibronic absorption spectra (Figure 2a) is that the spectral shape is affected by the specific monomer considered, although to a lesser extent than anticipated. In fact, the overall shape is well conserved and, with the chosen convolution, it is dominated by a progression with an apparent step of about 1400-1500 cm^{-1}. The two modes most contributing to such progression are the first two effective modes. Each of them represents a ring-breathing mode[50,70] concentrated on the inner rings of one of the two monomers (ESI, Figure S4) and their frequencies ω_1 are very similar for all the **Tn$_2$** dimers, while their linear couplings λ_1 decrease moderately with **n** (Table 1). The most noticeable effect of increasing the number of units **n** is the obvious red-shift of the vertical transition of the monomers, accompanied by an overall intensity increase.[47,55] A slow convergence of the S0-S1 excitation energies is observed (Figures 2a and S3, ESI), in keeping with literature.[55,71-73] The vertical S0-S1 excitation energy calculated for our longest model (**T13**) is 2.56 eV, while the value extrapolated for the long-chain limit using W. Kuhn's fit model[74,75] is 2.45 eV.‡

A second apparent effect of varying the chain length is a redistribution of the relative intensities of the vibronic bands, the second of which (starting from the low energy side) becomes relatively more intense in the absorption spectra (Figure 2a) and less intense in the ECD spectra (Figure 2b) upon increasing **n**. ECD spectra appear in all cases as positive couplets (i.e., a positive low-energy band followed by a negative high-energy band), in keeping with the expectation from exciton theory for a positive twist angle θ.[9] However, the vibronic pattern strongly alters the spectral shape with respect to a purely electronic couplet.[76] In the ECD spectra the effect of the chain length is also appreciated. In fact, the lowest energy negative vibronic band, which is almost absent or appears as a shoulder for small models (**T3$_2$** and **T5$_2$**, Figure 2b), is clearly distinguishable for medium-length models (**T7$_2$**) and finally becomes the strongest negative band for the longest model (**T13$_2$**).

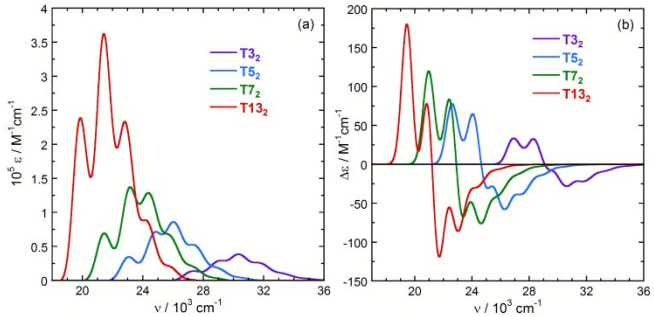

Fig. 2 Calculated vibronic absorption (a) and ECD spectra (b) for dimers **T3$_2$**, **T5$_2$**, **T7$_2$** and **T13$_2$** at r= 5 Å and θ= 15°, corresponding to the coupling potentials V_{12} listed in Table 1. Vibronic spectra convoluted with HWHM = 450 cm^{-1}, 6 effective modes included.

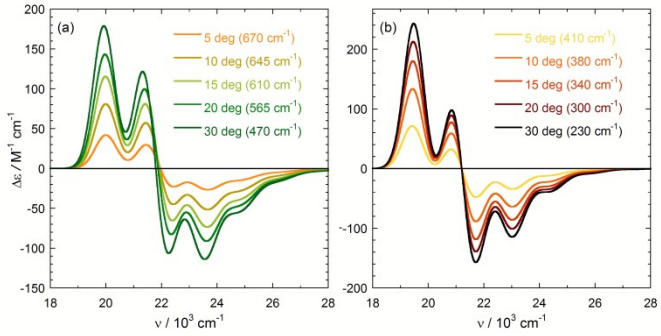

Fig. 3 Calculated vibronic ECD spectra for dimers **T7$_2$** (a) and **T13$_2$** (b) as a function of the coupling potentials V_{12} (given in parentheses). This latter corresponds to the indicated θ angles at a distance r= 5 Å. Spectra convoluted with HWHM = 450 cm^{-1}, 6 effective modes included.

Since in our model the normal modes are computed on the monomers **Tn**, the impact of the dimer geometry on the lineshape of the ECD spectra may be inferred by varying V_{12} (which depends on r and θ), as shown in Figure 3 for dimers **T7$_2$** and **T13$_2$** (the corresponding absorption spectra are given in Figures S9-S10 of the ESI; ECD and absorption spectra of **T3$_2$** and **T5$_2$** are reported in Figures S11-S12). We observe that while the ECD intensity varies almost linearly with V_{12}, the

overall shape is well preserved, with some variation observed only near to the crossover point for the short models. This is a surprising result, because a strong dependence of ECD spectra on the specific geometry adopted in the aggregates is in general expected.[9] In the current case, the spectral shape depends primarily on the vibrational progression of each single PT chain and is marginally affected by the inter-chain coupling. For example, the apparent couplet amplitude – the energy difference between the first positive and first negative peaks – is consistently between 2250-2450 cm^{-1} for both **T7$_2$** and **T13$_2$**; similar values are obtained for other dimers. This splitting between the two exciton components, which is normally a very informative parameter,[77] is here almost cancelled by the vibronic progression. The electronic coupling potential V_{12} estimated for **Tn$_2$** model dimers is (much) smaller than the vibrational spacing, a condition known as weak-coupling regime,[76] while the vibrational linear coupling λ_1 is sizeable (Table 1). As an immediate consequence, it is almost impossible to estimate V_{12} from a simple inspection of ECD spectra, as suggested e.g. by Janssen and co-workers.[17,19] In summary, the comparison of Figure 2 and 3 suggests that the details of the vibronic structure of the ECD spectrum are more affected by the chain length than by the inter-chain orientation in the dimer, or, in terms of parameters of the model, more by the vibrational couplings than by the electronic coupling V_{12}. In particular, the dependence on the linear coupling λ_1 of the first effective mode can be demonstrated by running a vibronic calculation on, e.g., **T13$_2$** and imposing a value of λ_1 corresponding to a shorter chain, e.g. **T5** (that is, 2558 instead of 2221 cm^{-1}, see Table 1). The resulting vibronic absorption and ECD spectra (see Figure S13, ESI) are very similar to those calculated for **T5$_2$**. Generally speaking, calculated absorption spectra on **Tn$_2$** dimers as a function of V_{12} (or of angle θ, at fixed r) showed a more pronounced variation than ECD (see ESI, Figures S9-S12). In fact, absorption (as well emission) spectra of aggregated PTs are known to be very sensitive to inter-chain interactions, and have received much attention as a source of information such as supramolecular structure, order and regularity.[5,46,50]

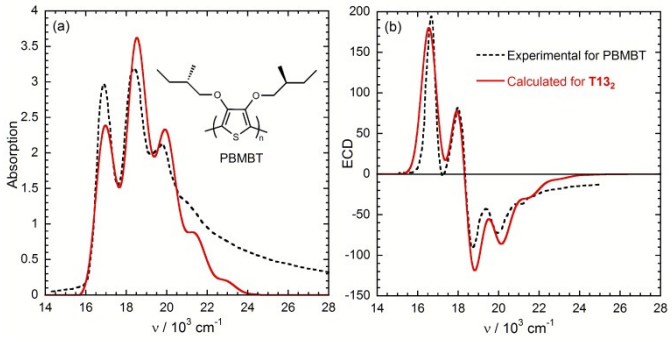

Fig. 4 Comparison between experimental absorption (a) and ECD spectra (b) of PBMBT (inset) in CH_2Cl_2 at 243K, and calculated spectra for dimer **T13$_2$** with r= 5 Å and θ= 15° (V_{12} = 340 cm^{-1}). Vibronic spectra convoluted with HWHM = 450 cm^{-1}; 6 effective modes included; shifted by –2900 cm^{-1}. Experimental spectra reprinted from ref. 19, with permission from Elsevier. Vertical axes are ε and Δε / $M^{-1}cm^{-1}$ for the calculations, while experimental spectra (provided as OD and mdeg) were scaled arbitrarily.

To check our calculation results against the experiment, we chose poly[3,4-bis((*S*)-2-methylbutoxy)thiophene] (PBMBT, inset in Figure 4). For this polymer a representative set of experimental spectra is available,[19] corresponding to different conditions used to promote aggregation, such as film deposition, use of a "poor solvent" or low temperatures. In particular, solution aggregates obtained at low temperature in CH_2Cl_2 and 2-methyl THF showed the best-resolved vibronic ECD spectra, very similar to each other.[19] In Figure 4 we compare the spectrum in CH_2Cl_2 at 243K with the results for dimer **T13$_2$**; the geometrical parameters were kept at r= 5 Å and θ= 15°. Both the experimental absorption and ECD profiles are reproduced very well by the computed spectra, apart from the obvious blue-shift due to the use of finite oligomers discussed before. The use of our largest model is expected to mimic better the behaviour of long chains of PBMBT (batch with M_w≈ 15 kDa) in conditions of high order and regularity as those promoted by low temperature in solution.[19] However, we observe that ECD spectra measured on thin films of PBMBT, i.e. conditions leading to larger disorder and shorter conjugation lengths, are even better reproduced by a smaller model such as **T5$_2$** (see ESI, Figure S14). The remarkable agreement observed in Figure 4 was in part unexpected in consideration of the crude model used for the aggregate. Several reports demonstrate in fact that, in ordered chiral supramolecular assemblies of chromophoric entities, long-range exciton couplings, i.e. couplings between non-immediate neighbours, may bring about a very strong contribution to the final ECD spectrum.[78-81] This is however primarily true for two quantities, namely the coupling potential and the spectrum intensity, which – for different reasons – are not an issue in the present case. In fact, the true experimental normalized ECD intensity is often unknown for polymer aggregates, while the impact of the coupling potential is masked by the vibrational progression, as discussed above. Thus, the apparent effectiveness of a simple dimeric model for PTs may be ascribed to the peculiar nature of vibronic excitonic ECD spectra in the weak-coupling regime, and not to the fact that first-neighbour or short-range couplings are dominant.[82,83]

Conclusions

The main result from our study is that vibronic ECD spectra of PT aggregates offer a unique fingerprint of the presence of a chiral supramolecular structure in solution or thin film. The appearance of vibronic ECD spectra similar to those shown in Figure 4 is an immediate proof of the formation of chiral aggregates of quasi-planar PT chains arranged almost parallel to each other with some tilt angle.[19] This conclusion clearly supports the widespread use of ECD as a diagnostic tool to monitor PT aggregation in various conditions. On the contrary, the geometry dependence of the ECD spectra is less pronounced than anticipated and commonly believed. In our model, the vibrational progression of each oligothiophene monomer (an intra-chain effect) is the major factor determining the final shape of the vibronic ECD spectrum of

the dimer, and dominates over the exciton coupling (an inter-chain effect). Thus, a detailed analysis of absorption and emission band-shapes should be preferred to extract quantitative structural parameters.[5,46,50,63]

From a more fundamental viewpoint, our results demonstrate that the use of a relatively small molecular model for PT aggregates is sufficient to get a reasonable picture of the vibronic exciton coupling between aggregated PT chains, at least in terms of the shape of the ECD spectra. This is because in the weak-coupling regime the overall band-shape is mostly determined by the intrinsic monomer vibronic band-shape and therefore less affected by long-distance couplings, which would need much larger models to be correctly predicted.

Finally, we notice that our model can be easily extended to other chiral conjugated polymers. In particular, chiral poly(p-phenyleneethynylene)s (PPEs) show distinct aggregate ECD spectra, often with recognizable vibronic features,[67,84-86] whose origin is still debated in the literature with respect to the inter-chain vs. intra-chain origin and the role of ring librations.[87]

Acknowledgments

We gratefully thank Prof. Lorenzo Di Bari, Prof. Petr Bouř, Dr. Javier Cerezo and David Picconi for fruitful discussions, and IOCB Postdoctoral Fellowship and MIUR-PRIN projects n. 2012A4Z2RY and 2010ERFKXL for funding.

Notes and References

‡ This latter value can be compared with reference values (around 2.0 eV) obtained with TDDFT method and using the same fitting procedure.[71,73,74] The discrepancy with our value is largely due to the use of two different functionals,[88] namely the range-separated CAM-B3LYP in our case, and the global hybrid B3LYP in all other quoted examples. CAM-B3LYP was a necessary choice here to avoid the occurrence of spurious charge-transfer states in the stacked dimers. Moreover, the analysis in ref. 47 suggests that including the solvent effects and increasing the basis set predicts very accurate absolute energies, at least on small PT oligomers (up to **T7**).

1 X. Guo, M. Baumgarten and K. Müllen, *Progr. Polym. Sci.*, 2013, **38**, 1832-1908.
2 P. M. Beaujuge and J. M. J. Fréchet, *J. Am. Chem. Soc.*, 2011, **133**, 20009-20029.
3 Z. B. Henson, K. Mullen and G. C. Bazan, *Nat. Chem.*, 2012, **4**, 699-704.
4 F. J. M. Hoeben, P. Jonkheijm, E. W. Meijer and A. P. H. J. Schenning, *Chem. Rev.*, 2005, **105**, 1491-1546.
5 A. Salleo, R. J. Kline, D. M. DeLongchamp and M. L. Chabinyc, *Adv. Mater.*, 2010, **22**, 3812-3838.
6 L. Pu, *Acta Polym.*, 1997, **48**, 116-141.
7 L. A. P. Kane-Maguire and G. G. Wallace, *Chem. Soc. Rev.*, 2010, **39**, 2545-2576.
8 M. Verswyvel and G. Koeckelberghs, *Polym. Chem.*, 2012, **3**, 3203-3216.
9 G. Pescitelli, L. Di Bari and N. Berova, *Chem. Soc. Rev.*, 2014, **43**, 5211-5233.
10 P. A. Korevaar, T. F. A. de Greef and E. W. Meijer, *Chem. Mater.*, 2013, **26**, 576-586.
11 N. Berova, L. Di Bari and G. Pescitelli, *Chem. Soc. Rev.*, 2007, **36**, 914-931.
12 M. Jeffries-El and R. D. McCullogh, in *Handbook of Conducting Polymers*, eds. T. A. Skotheim and J. R. Reynolds, CRC Press, New York, 2007, pp. 9.1-9.49.
13 D. Fichou, ed., *Handbook of Oligo- and Polythiophenes*, Wiley-VCH, Weinheim, 1999.
14 T. Shiraki, A. Dawn, Y. Tsuchiya, T. Yamamoto and S. Shinkai, *Chem. Commun.*, 2012, **48**, 7091-7093.
15 H. Goto, Y. Okamoto and E. Yashima, *Chem. Eur. J.*, 2002, **8**, 4027-4036.
16 H. Goto, Y. Okamoto and E. Yashima, *Macromolecules*, 2002, **35**, 4590-4601.
17 B. M. W. Langeveld-Voss, D. Beljonne, Z. Shuai, R. A. J. Janssen, S. C. J. Meskers, E. W. Meijer and J.-L. Brédas, *Adv. Mater.*, 1998, **10**, 1343-1348.
18 B. M. W. Langeveld-Voss, E. Peeters, R. A. J. Janssen and E. W. Meijer, *Synth. Met.*, 1997, **84**, 611-614.
19 B. M. W. Langeveld-Voss, R. A. J. Janssen and E. W. Meijer, *J. Mol. Struct.*, 2000, **521**, 285-301.
20 C. R. G. Grenier, S. J. George, T. J. Joncheray, E. W. Meijer and J. R. Reynolds, *J. Am. Chem. Soc.*, 2007, **129**, 10694-10699.
21 T. Minami and Y. Kubo, *Supramol. Chem.*, 2011, **23**, 13-18.
22 K. Watanabe, I. Osaka, S. Yorozuya and K. Akagi, *Chem. Mater.*, 2012, **24**, 1011-1024.
23 B. M. W. Langeveld-Voss, R. A. J. Janssen, M. P. T. Christiaans, S. C. J. Meskers, H. P. J. M. Dekkers and E. W. Meijer, *J. Am. Chem. Soc.*, 1996, **118**, 4908-4909.
24 M. M. Bouman and E. W. Meijer, *Adv. Mater.*, 1995, **7**, 385-387.
25 G. Bidan, S. Guillerez and V. Sorokin, *Adv. Mater.*, 1996, **8**, 157-160.
26 B. M. W. Langeveld-Voss, R. J. M. Waterval, R. A. J. Janssen and E. W. Meijer, *Macromolecules*, 1999, **32**, 227-230.
27 Y. Takeoka, F. Saito and M. Rikukawa, *Langmuir*, 2013, **29**, 8718-8727.
28 F. Brustolin, F. Goldoni, E. W. Meijer and N. A. J. M. Sommerdijk, *Macromolecules*, 2002, **35**, 1054-1059.
29 C. Li , M. Numata, M. Takeuchi and S. Shinkai *Chem. Asian J.*, 2006, **1**, 95-101.
30 M. Catellani, S. Luzzati, F. Bertini, A. Bolognesi, F. Lebon, G. Longhi, S. Abbate, A. Famulari and S. V. Meille, *Chem. Mater.*, 2002, **14**, 4819-4826.
31 F. Lebon, G. Longhi, S. Abbate, M. Catellani, F. Wang and P. L. Polavarapu, *Enantiomer*, 2002, **7**, 207-212.
32 H. Goto, Y. Yokochi and E. Yashima, *Chem. Commun.*, 2012, **48**, 3291-3293.
33 K. P. R. Nilsson, J. D. M. Olsson, P. Konradsson and O. Inganäs, *Macromolecules*, 2004, **37**, 6316-6321.

34 K. P. R. Nilsson, M. R. Andersson and O. Inganäs, *Synth. Met.*, 2003, **135–136**, 291-292.
35 Z.-B. Zhang, M. Fujiki, M. Motonaga, H. Nakashima, K. Torimitsu and H.-Z. Tang, *Macromolecules*, 2002, **35**, 941-944.
36 E. Salatelli, L. Angiolini and A. Brazzi, *Chirality*, 2010, **22**, E74-E80.
37 A. Wang, K. Kawabata and H. Goto, *Des. Monomers Polym.*, 2015, **18**, 360-366.
38 C. Taliani and W. Gebauer, in *Handbook of Oligo- and Polythiophenes*, ed. D. Fichou, Wiley-VCH, Weinheim, 1999.
39 M. Verswyvel, K. Goossens and G. Koeckelberghs, *Polym. Chem.*, 2013, **4**, 5310-5320.
40 H. Peeters, P. Couturon, S. Vandeleene, D. Moerman, P. Leclere, R. Lazzaroni, I. D. Cat, S. D. Feyter and G. Koeckelberghs, *RSC Adv.*, 2013, **3**, 3342-3351.
41 M. M. Bouman, E. E. Havinga, R. A. J. Janssen and E. W. Meijer, *Mol. Cryst. Liq. Cryst. Sci. Technol., Sect. A*, 1994, **256**, 439-448.
42 K. Van den Bergh, I. Cosemans, T. Verbiest and G. Koeckelberghs, *Macromolecules*, 2010, **43**, 3794-3800.
43 K. Van den Bergh, J. Huybrechts, T. Verbiest and G. Koeckelberghs, *Chem. Eur. J.*, 2008, **14**, 9122-9125.
44 P. Willot, J. Steverlynck, D. Moerman, P. Leclere, R. Lazzaroni and G. Koeckelberghs, *Polym. Chem.*, 2013, **4**, 2662-2671.
45 D. Padula, D. Picconi, A. Lami, G. Pescitelli and F. Santoro, *J. Phys. Chem. A*, 2013, **117**, 3355-3368.
46 F. C. Spano and C. Silva, *Annu. Rev. Phys. Chem.*, 2014, **65**, 477-500.
47 R. Improta, F. J. A. Ferrer, E. Stendardo and F. Santoro, *ChemPhysChem*, 2014, **15**, 3320-3333.
48 H. Yamagata and F. C. Spano, *J. Chem. Phys.*, 2012, **136**, 184901.
49 J. Clark, C. Silva, R. H. Friend and F. C. Spano, *Phys. Rev. Lett.*, 2007, **98**, 206406.
50 P. J. Brown, D. S. Thomas, A. Köhler, J. S. Wilson, J.-S. Kim, C. M. Ramsdale, H. Sirringhaus and R. H. Friend, *Phys. Rev. B*, 2003, **67**, 064203.
51 F. C. Spano, *Chem. Phys.*, 2006, **325**, 22-35.
52 F. Panzer, M. Sommer, H. Bässler, M. Thelakkat and A. Köhler, *Macromolecules*, 2015, **48**, 1543-1553.
53 D. Iarossi, A. Mucci, F. Parenti, L. Schenetti, R. Seeber, C. Zanardi, A. Forni and M. Tonelli, *Chem. Eur. J.*, 2001, **7**, 676-685.
54 E. Peelers, R. A. J. Janssen and E. W. Meijer, *Synth. Met.*, 1999, **102**, 1105-1106.
55 H. Sun and J. Autschbach, *J. Chem. Theory Comput.*, 2014, **10**, 1035-1047.
56 R. Colle, G. Grosso, A. Ronzani and C. M. Zicovich-Wilson, *Phys. Status Solidi B*, 2011, **248**, 1360-1368.
57 A. A. Voityuk, *J. Chem. Phys.*, 2014, **140**, 244117.
58 B. P. Krueger, G. D. Scholes and G. R. Fleming, *J. Phys. Chem. B*, 1998, **102**, 5378-5386.
59 J. Gierschner, Y.-S. Huang, B. Van Averbeke, J. Cornil, R. H. Friend and D. Beljonne, *J. Chem. Phys.*, 2009, **130**, 044105.
60 M. Muccini, M. Schneider, C. Taliani, M. Sokolowski, E. Umbach, D. Beljonne, J. Cornil and J. L. Brédas, *Phys. Rev. B*, 2000, **62**, 6296-6300.
61 S. Westenhoff, A. Abrusci, W. J. Feast, O. Henze, A. F. M. Kilbinger, A. P. H. J. Schenning and C. Silva, *Adv. Mater.*, 2006, **18**, 1281-1285.
62 D. Beljonne, J. Cornil, R. Silbey, P. Millié and J. L. Brédas, *J. Chem. Phys.*, 2000, **112**, 4749-4758.
63 C. Scharsich, R. H. Lohwasser, M. Sommer, U. Asawapirom, U. Scherf, M. Thelakkat, D. Neher and A. Köhler, *J. Polym. Sci., Part B: Polym. Phys.*, 2012, **50**, 442-453.
64 D. Picconi, A. Lami and F. Santoro, *J. Chem. Phys.*, 2012, **136**, 244104.
65 L. S. Cederbaum, E. Gindensperger and I. Burghardt, *Phys. Rev. Lett.*, 2005, **94**, 113003.
66 M. Pawlikowski and M. Z. Zgierski, *J. Chem. Phys.*, 1982, **76**, 4789-4797.
67 S. Zahn and T. M. Swager, *Angew. Chem. Int. Ed.*, 2002, **41**, 4225-4230.
68 F. Babudri, D. Colangiuli, L. Di Bari, G. M. Farinola, O. Hassan Omar, F. Naso and G. Pescitelli, *Macromolecules*, 2006, **39**, 5206-5212.
69 J. Seibt and V. Engel, *J. Chem. Phys.*, 2007, **126**, 074110.
70 J. H. Schön, C. Kloc, R. A. Laudise and B. Batlogg, *J. Appl. Phys.*, 1999, **85**, 2844-2847.
71 S. S. Zade and M. Bendikov, *Org. Lett.*, 2006, **8**, 5243-5246.
72 U. Salzner, *J. Chem. Theory Comput.*, 2007, **3**, 1143-1157.
73 J. Gierschner, J. Cornil and H. J. Egelhaaf, *Adv. Mater.*, 2007, **19**, 173-191.
74 J. Torras, J. Casanovas and C. Alemán, *J. Phys. Chem. A*, 2012, **116**, 7571-7583.
75 K. R. Naqvi, *J. Phys. Chem. Lett.*, 2016, **7**, 676-679.
76 O. E. Weigang, *J. Chem. Phys.*, 1965, **43**, 71-72.
77 L. Di Bari, G. Pescitelli and P. Salvadori, *J. Am. Chem. Soc.*, 1999, **121**, 7998-8004.
78 L. van Dijk, P. A. Bobbert and F. C. Spano, *J. Phys. Chem. B*, 2010, **114**, 817-825.
79 B. Nieto-Ortega, J. Casado, J. T. López Navarrete, G. Hennrich and F. J. Ramírez, *J. Chem. Theory Comput.*, 2011, **7**, 3314-3322.
80 F. D. Lewis, X. Liu, Y. Wu and X. Zuo, *J. Am. Chem. Soc.*, 2003, **125**, 12729-12731.
81 P. Norman and M. Linares, *Chirality*, 2014, **26**, 483-489.
82 S. Masiero, R. Trotta, S. Pieraccini, S. De Tito, R. Perone, A. Randazzo and G. P. Spada, *Org. Biol. Chem.*, 2010, **8**, 2683-2692.
83 D. Padula, S. D. Pietro, M. A. M. Capozzi, C. Cardellicchio and G. Pescitelli, *Chirality*, 2014, **26**, 462-470.
84 G. Pescitelli, O. H. Omar, A. Operamolla, G. M. Farinola and L. Di Bari, *Macromolecules*, 2012, **45**, 9626-9630.
85 J. V. Prata, A. I. Costa, G. Pescitelli and H. D. Pinto, *Polym. Chem.*, 2014.
86 C. Resta, G. Pescitelli and L. Di Bari, *Macromolecules*, 2014, **47**, 7052-7059.
87 U. H. F. Bunz, *Macromol. Rapid Commun.*, 2009, **30**, 772-805.

88 D. Jacquemin, E. A. Perpète, G. E. Scuseria, I. Ciofini and C. Adamo, *J. Chem. Theory Comput.*, 2008, **4**, 123-135.

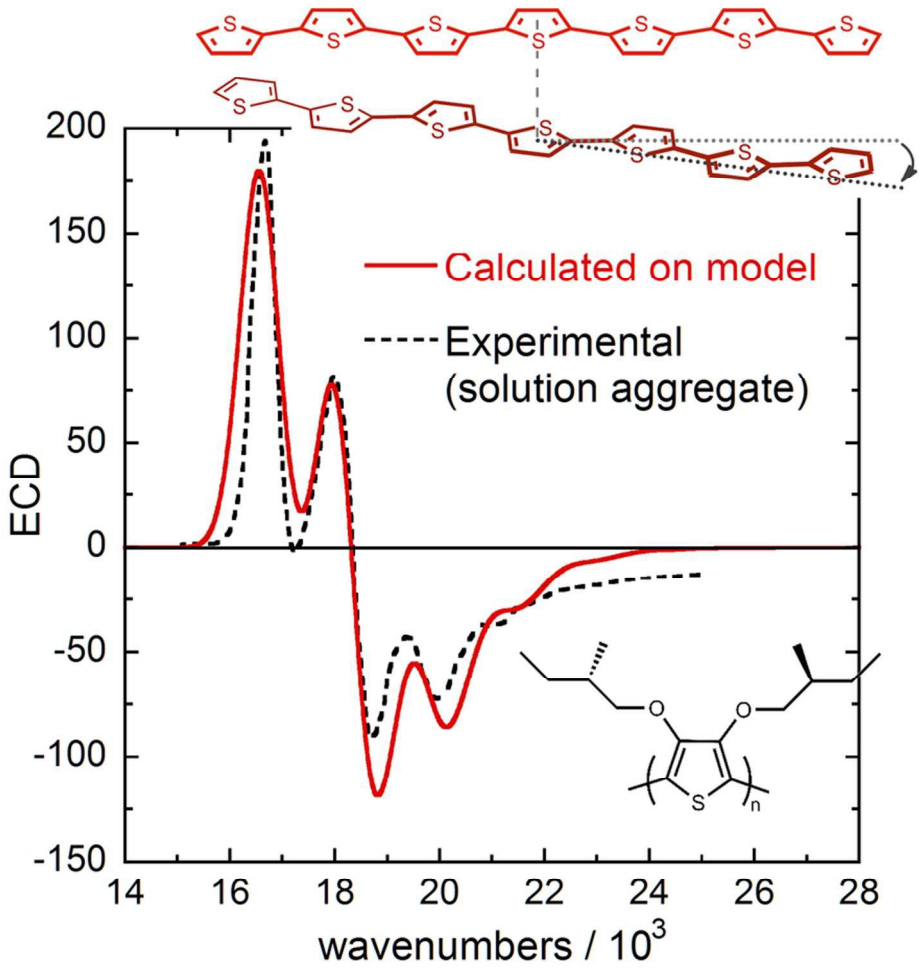

81x81mm (300 x 300 DPI)